Available online at www.sciencedirect.com
ScienceDirect
Acta Materialia 58 (2010) 606–614
Acta MATERIALIA
www.elsevier.com/locate/actamat

Wettability of pure Ti by molten pure Mg droplets

Katsuyoshi Kondoh *, Masashi Kawakami, Hisashi Imai, Junko Umeda, Hidetoshi Fujii

Joining and Welding Research Institute, Osaka University, 11-1, Mihogaoka, Ibaragi, Osaka 567-0047, Japan

Received 2 May 2009; received in revised form 20 September 2009; accepted 21 September 2009
Available online 21 October 2009

Abstract

The wetting behavior of molten pure Mg droplets on pure Ti substrate, a crucial phenomenon in the design of Mg matrix composites reinforced with Ti particles, was investigated by the sessile drop method. The contact angle was measured in high-purity argon (99.999%) at 1073 K. In particular, the effects of two important parameters on the contact angle were evaluated: Mg evaporation during the wetting test; and surface oxide film of the substrate. The calculation method to estimate the modified contact angle involved taking the morphological changes of the droplet outline due to the evaporation into consideration. By changing the thickness of the surface oxide films on the Ti substrate, it was possible to examine the wettability and the chemical reactions at the interface between the solidified Mg drop and the substrate were investigated by scanning electron microscopy–energy dispersive X-ray spectrometry analysis. At the initial wetting stage, a large contact angle with 95–110° was obtained, which depended on the reduction of TiO_2 surface films by Mg droplets. When the molten Mg contacts an area of pure Ti after reduction, the contact angle suddenly decreased. The equilibrium value at the stable state strongly depended on the surface roughness of the Ti plate.

Keywords: Pure magnesium; Titanium; Contact angle; Young's equation; Evaporation

1. Introduction

Mg alloys have important advantages due to their high specific strength. However, an enhanced Young's modulus is a necessity for Mg alloys intended for use as structural components. For example, ceramic particulates such as SiC, TiC, and Al_2O_3, are useful reinforcements to improve the stiffness of Mg matrix composites [1–5]. The inevitable disadvantage of adding ceramic reinforcements is a decrease in the ductility of the composite. When designing Mg matrix composites with high strength and good ductility, the Ti particles are an effective reinforcement because Ti and its alloys have high Young's modulus, hardness and sufficient elongation [6,7] compared to Mg alloys. Previous studies have reported that particles of Ti and its alloys dispersed in the matrix of Mg composites [8–10] were useful reinforcement, improving not only the tensile strength but also the elongation at room temperature. In general, the wetting behavior of the reinforcement surface by the molten matrix metal is one of the most important phenomena to consider when fabricating composites [11,12]. This is because the creation of a good bond between the dispersoids and the matrix depends critically on the wetting behavior. The wetting of a solid by a liquid (molten metal) depends on the relationship between the interfacial tensions for the three phases: solid/liquid (SL), liquid/vapor (LV) and solid/vapor (SV). The contact angle for a molten metal on the substrate with a smooth surface is described by Young's equation [13] as follows;$\cos\theta = (\gamma_{SV} - \gamma_{SL})/\gamma_{LV}$where θ is the contact angle, and γ_{SL}, γ_{LV} and γ_{SV} are the interfacial energies per unit area for the SL, LV and SV interfaces, respectively. A few experimental studies using the above equation have been carried out on the wettability of ceramics by Al, Mg and their alloys [14–16], but not pure by Ti, by using the sessile drop technique. In addition, when discussing wetting by molten Mg, the effects of its evaporation should be taken into consideration because of its high evaporation pressure. A previous study investigated the influence of Mg evaporation on the wettability of MgO by pure Mg droplets at high temperature

* Corresponding author. Tel.: +81 06 6879 4369.
E-mail address: kondoh@jwri.osaka-u.ac.jp (K. Kondoh).

1359-6454/$36.00
doi:10.1016/j.actamat.2009.09.039

[16], but made no effort to quantitatively discuss the Mg vaporization effect on the contact angle during wetting. Furthermore, the reduction of the surface oxide films of the substrate metal by molten Mg droplets possibly affects the wettability [14]. Accordingly, when designing Mg matrix composites reinforced with Ti particles, it is very important to discuss the wettability of pure Mg on pure Ti substrate at high temperatures because Ti is an active metals and TiO_2 films are easily formed on the Ti surface.

This investigation quantitatively evaluates the effect of Mg evaporation on the contact angle between molten pure Mg droplets and Ti substrate at 1073 K in argon by the sessile drop method. The influence of the surface oxide films of the substrate on the wettability is investigated for both as-received Ti plates and for plates coated with thicker oxide films after heat treatment in air. TiO_2 ceramic plate is also employed as the substrate in the wettability evaluation to discuss the reduction behavior by molten Mg during wetting. In particular, morphological and chemical changes in the surface of pure Ti substrate after reduction are investigated by scanning electron microscopy–energy-dispersive X-ray spectrometry (SEM–EDS) and electron probe microanalysis (EPMA) of the interface between pure Mg droplets and the substrate to evaluate the chemical reactions that occur during wetting. Finally, the wetting mechanism of pure Ti by molten pure Mg is clarified, and its wettability is evaluated in comparison with the combination of pure Mg with conventional ceramics such as SiC and TiC.

2. Materials and methods

The sessile drop method [17] was used to study the wetting behavior of molten pure Mg droplets on pure Ti substrate. The contact angle for an Mg droplet, indicating its wettability, is calculated using Young's equation as mentioned above. Fig. 1 illustrates a schematic diagram of the experimental equipment used to evaluate the wettability in this study. The raw material used was pure Mg rod (99.98%); 20 mm × 20 mm pure Ti plate (99.835%), 3 mm thick and with a smooth polished surface with roughness of 63–67 nm, was used as the substrate. The contents of the impurities are as follows: O, 0.075; Fe, 0.052; H, 0.032; C, 0.004; N, 0.002 (mass%). This equipment consists of a Mo reflector installed in the sealed chamber, a carbon heater, a MgO dropping tube, a *K*-type thermocouple, an evacuating pump system, He–Ne lasers (wavelength 632.8 nm), and high-resolution digital cameras with band-pass filters passing only 632 nm laser beam. Two sets of the digital camera and He–Ne laser system were installed to evaluate the symmetry of the molten Mg droplet on the substrate. For example, Fig. 2 shows the changes in the height and diameter of the pure Mg droplet on pure Ti plate at 1073 K measured by two digital cameras (0° and 90° direction). There is no significant difference in the height and diameter between the measurements in different directions. This means molten Mg droplets on the

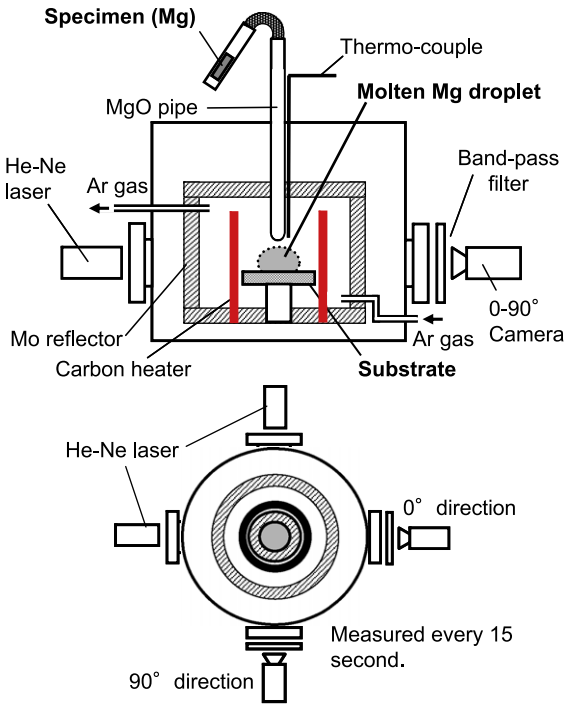

Fig. 1. Schematic illustration of sessile drop test equipment to evaluate wettability of pure Ti by molten pure Mg at high temperature.

substrate have a morphological symmetry during wetting. After evacuating the chamber to about 1×10^{-3} Pa, and the chamber was heated up to 1073 K at a heating rate of 20 K min^{-1}. Subsequently, high-purity argon (99.999%) was flowed into the chamber. The thermocouple was positioned beside the MgO dropping tube to measure the temperature of the melt Mg in the tube. To correct the temperature measurement, a pure Ag molten droplet was placed on pure Fe substrate. This is because the melting point of high-purity Ag is constant (1234.9 K), and molten Ag does not react with pure Fe. After keeping the MgO tube at 1073 K for 120 s, the molten pure Mg was dropped on the Ti substrate through the hole at the bottom of the MgO tube. At the same time, pictures of the outline of the Mg droplet were taken every 15 s by the digital cameras from two directions. The initial oxide films coating the raw Mg rod were removed by passing through the above small 1 mm diameter hole. To calculate the contact angle between the droplet and the substrate, the axisymmetric-drop-shape-analysis program was applied to the photographs captured by a computer. In order to investigate the effect of surface oxide films of the pure Ti substrate on the wetting behavior, TiO_2 ceramic plate (98.2%) and pure Ti substrate annealed at 773 K for 3.6 ks in air were prepared. The thickness of the TiO_2 films of the annealed Ti plate was measured by Auger electron spectroscopy (AES, ULVAC-PHI, Inc. PHI700) analysis with a sputtering level of 2.2 nm min^{-1}. SEM (JEOL JSM-6500F) with EDS (JEOL JED-2300) and EPMA (JEOL JXA-8600F) were used to investigate the chemical reaction at the interface between the solidified Mg drop and the Ti or TiO_2 substrate.

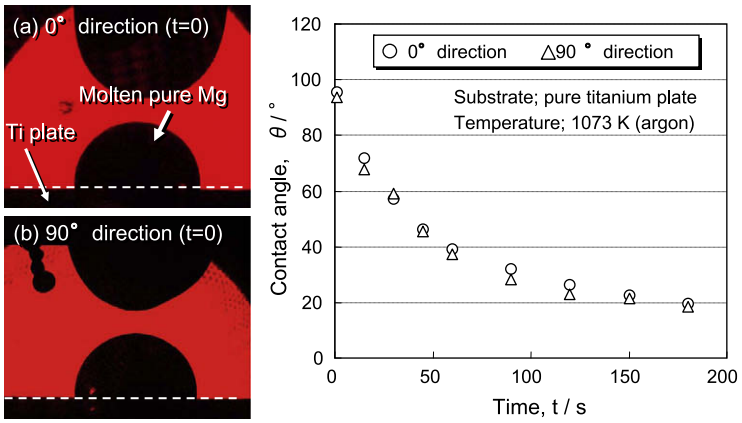

Fig. 2. Evaluation of morphological symmetry of pure Mg molten droplet on pure Ti substrate. Changes in contact angle of molten pure Mg droplet on pure Ti plate at 1073 K measured at 0°and 90° directions.

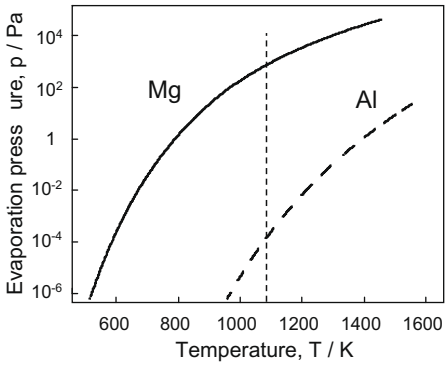

Fig. 3. Evaporation pressure of pure Mg and pure Al as a function of temperature.

3. Results and discussion

3.1. Estimation of Mg vaporization effect on contact angle

Mg has a very high evaporation pressure compared to Al and other metal elements, except Zn [18,19]. Fig. 3 shows the variation of the evaporation pressure of pure Mg and pure Al as a function of temperature [20]. The evaporation pressure of Mg and Al at 1073 K is 2.00×10^{3} and 3.87×10^{-3} Pa, respectively. This means that evaporation of Mg from its molten droplet readily occurs during the wetting test at 1073 K. Therefore, the evaporation behavior of Mg should be taken into consideration when discussing the wetting phenomenon of pure Mg and calculating the contact angle at high temperature over its melting point (923 K). As schematically illustrated in Fig. 4, the Mg dropped on the substrate has an initial contact angle, θ_0 at $t = 0$, and its diameter and height are D_0 and H_0, respectively. On the assumption that the molten metal has a very poor wettability on the substrate, no change in the diameter of the droplet ($D_1 = D_0$) occurs after t_1. However, the height decreases ($H_1 < H_0$) due to the vaporization of the metal from the molten droplet. As a result, the contact angle θ_1 at $t = t_1$ becomes smaller than the initial value (θ_0), although wetting never occurs. Therefore, it is important to quantitatively estimate the effect of the volumetric change of the Mg droplet due to its evaporation on the contact angle. That is, the true con-

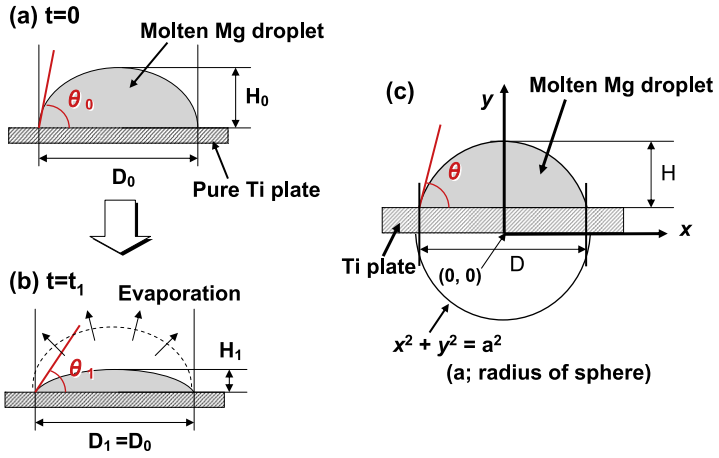

Fig. 4. Schematic illustration of morphological change of molten Mg droplet due to evaporation at high temperature (a and b), and diagram calculating droplet volume and contact angle with substrate using measurements of diameter and height of droplet (c).

tact angle should be calculated when discussing the wettability of pure Mg droplet on the substrate.

In calculating the volume of the pure Mg molten droplet on the Ti substrate as illustrated in Fig. 4c, it is assumed that the droplet is part of a sphere (radius a) and its contact angle is θ. The evaporation of Mg has no effect on the wetting phenomenon. The $x-y$ axes coordinate is schematically shown in the figure, and the two-dimensional droplet outline is expressed as $y=\sqrt{(a^2-x^2)}$. Then, the volume (V) of the Mg droplet (D, diameter; H, height) can be expressed as the following equation:

$$V=\int_{a-H}^{a}\left(\sqrt{a^2-x^2}\right)^2 dx=\frac{\pi H^2}{3}(3a-H) \tag{1}$$

Considering that $a=D/(2\sin\theta)$, the droplet volume is obtained as shown in the following equation:

$$V=\frac{\pi H^2}{6}\left(\frac{3D}{\sin\theta}-2H\right) \tag{2}$$

Fig. 5 shows a schematic diagram of the morphological change of pure Mg molten droplet on Ti substrate caused by both wetting and Mg evaporation at high temperature. Fig. 5a indicates the initial diameter and height of the droplet at $t=0$ are D_0 and H_0, respectively. At $t=t_1$ shown in Fig. 5b, the droplet diameter, D_1 is larger than D_0, and its height, H_1 is smaller than the initial value (H_0). These morphological changes of the droplet outline are due not only to the progress of the wetting phenomenon but also to Mg evaporation at high temperature. Accordingly, it is obvious that the evaporation strongly affects the contact angle, and a deceptive contact angle, θ_1 is obtained using the original measurements (D_1 and H_1). The dotted line corresponds to the droplet profile modified by adding the vaporized Mg volume for t_1, and the true contact angle is θ_1^*. The addition of an asterisk (*) on each characteristic indicates a modification due to consideration of the Mg evaporation behavior, and each value is calculated on the supposition that wetting, rather than evaporation of Mg, occurs during the wetting test. As shown in Fig. 5c, in order to estimate the true contact angle θ_t^* at $t=t$, the height of the modified outline (H_t^*) must be calculated. The assumption of no Mg evaporation indicates that the droplet volume is constant ($V_0=V_1^*=V_t^*$) and no volumetric change occurs even after the wetting test. For the calculation of H_t^*, by considering that $x^2+y^2=a^2$, $y=a-H$ and $x=D/2$, a function of the morphological parameters of the droplet (H, D, and a) is then obtained as follows:

$$H^2-2aH+\frac{D^2}{4}=0 \tag{3}$$

By Eq. (1), the radius (a) of the sphere shown in Fig. 4c is expressed in the following equation:

$$a=\frac{V}{\pi H^2}+\frac{H}{3} \tag{4}$$

According to Eqs. (3) and (4), the following is obtained:

$$H^3+\frac{3D^2H}{4}-\frac{6V}{\pi}=0 \tag{5}$$

As mentioned above, the droplet volume is constant, i.e. $V_t^*=V_0$ at any time. The droplet diameter (D_t) is a measured value, obtained experimentally via the digital camera. Therefore, by substituting these values for Eq. (5), the true height of the modified droplet (H_t^*) can be estimated. The modified radius (a_t^*) is also obtained by Eq. (4). As a result, the true contact angle, θ_t^* is expressed as follows:

$$\theta_t^*=\sin^{-1}\frac{D_t}{2a_t^*} \tag{6}$$

Fig. 6 shows photos of the morphological changes of the Mg droplet outline on pure Ti substrate at 1073 K in argon. With increasing time, the droplet diameter gradually increases, and its height is reduced. When comparing the droplet volume at $t=60$ s (b) and $t=420$ s (f), the former is obviously larger than that of the latter. This means that the remarkable evaporation of Mg occurs during the wetting test because of its very high evaporation pressure as mentioned above. Fig. 7a reveals the changes in the original height and diameter measured from the photos of the droplet outline shown in Fig. 6. The contact angle is calculated from these measurements. On the other hand, Fig. 7b shows the modified morphological parameters of the droplet and the true contact angle (θ^*) estimated by Eqs. (5) and (6) to consider the Mg evaporation effect. It indicates that the true contact angle between the pure Mg droplet and the pure Ti substrate at 1073 K in 180 s is about 31°, i.e. much smaller than 90°. When considering that the contact angle of pure Mg molten drops with TiC substrates is about 110° [15], the wettability of pure Ti by molten pure Mg is extre-

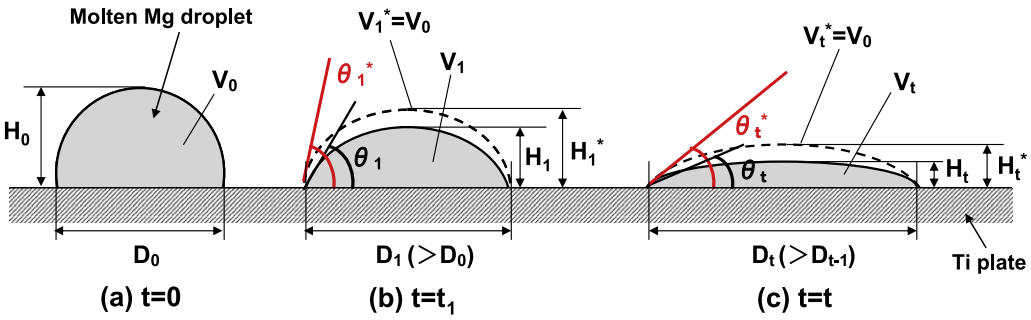

Fig. 5. Changes in diameter and height of Mg molten droplet and contact angle due to wetting phenomenon and Mg evaporation in wetting test.

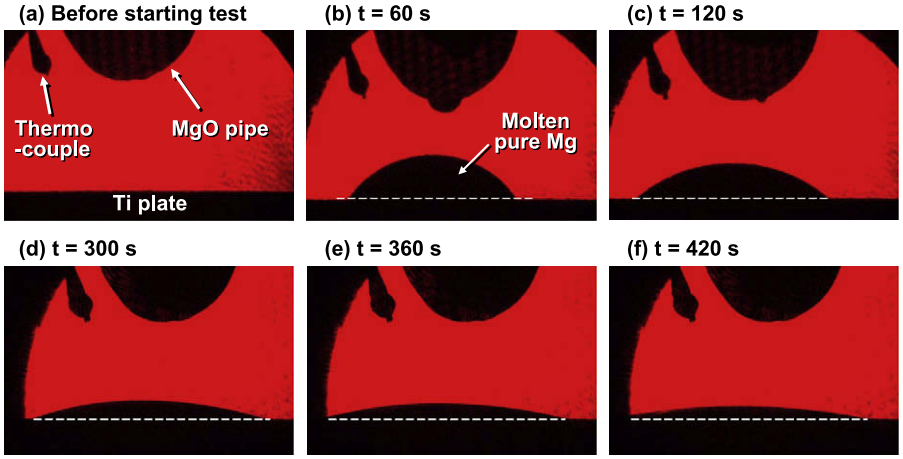

Fig. 6. Photos showing morphological changes of pure Mg molten droplet on pure Ti substrate at 1073 K in sessile drop test.

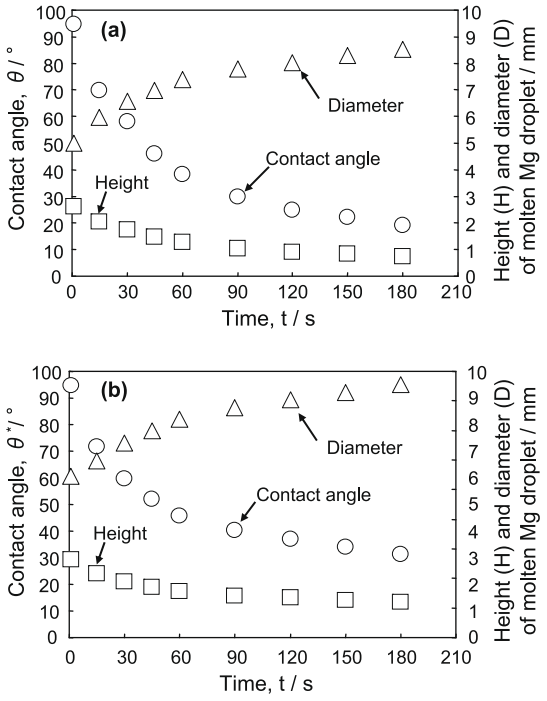

Fig. 7. Changes in contact angle, diameter and height of pure Mg molten droplet at 1073 K. Original data (a) and modified data considering Mg evaporation effect during wetting test (b).

mely good. Furthermore, the modification by considering the effect of Mg evaporation on the volumetric reduction of the droplet in wetting causes an increment of the contact angle of about 11° at 1073 K.

3.2. Effect of TiO_2 surface films on wettability

The residual oxygen gas pressure in the chamber was $P(O_2) = 1 \times 10^{-6}$ Pa. This indicates that there is very little residual oxygen, and a very small effect of magnesium oxide (MgO) on the molten Mg droplet. On the other hand, the residual oxygen gas is completely consumed by reaction with the evaporated Mg in the chamber. Therefore, it is not necessary to consider the effect of MgO on the wetting behavior at 1073 K, and the contact angle in the stabilized stage is the actual value between the molten pure Mg and the as-received Ti plate.

Concerning the effect of TiO_2 surface films on the wettability, in general, very thin TiO_2 films cover the surface of the Ti plate when operating in air. The wettability of pure Ti plate by molten Mg is controlled by several chemical and physical processes. In particular, the high reactivity of Mg causes the reaction with the oxides of the substrate. As shown in the following reactions [21,22], the reduction of TiO_2 (rutile) surface films by pure Mg easily takes place at 1073 K in argon.

$$\left.\begin{aligned} &2Mg + O_2 = 2MgO, \quad \Delta G_{Mg} = -983.4\ \mathrm{kJ}/[O_2]\mathrm{mol} \\ &Ti + O_2 = TiO_2, \quad \Delta G_{Ti} = -750.4\ \mathrm{kJ}/[O_2]\mathrm{mol} \\ &2Mg + TiO_2 = 2MgO + Ti, \\ &\Delta G = -233.0\ \mathrm{kJ/mol}(\Delta G, \text{standard free energy}) \end{aligned}\right\} \quad (7)$$

When the above reaction occurs, in situ formed MgO can chemically influence the wetting phenomenon at the interface between Ti substrate and the pure Mg molten droplet. Furthermore, it is expected that the surface roughness changes of the substrate caused by the above reaction will also have a significant effect on the wettability. In this study, in order to evaluate the effect of TiO_2 surface films on the pure Ti substrate, the plate was annealed at 773 K for 3.6 ks in air, and its surface was coated with thicker TiO_2 films. The surface is very smooth with a roughness of 61–66 nm, and the same as that of the as-received Ti plate (roughness range 63–67 nm). Fig. 8 indicates the appearance of the as-received pure Ti plate (a) and annealed plate (b), and EDS and AES analysis results on the surface of each plate are also indicated. Fig. 9 shows the X-ray diffraction (XRD) profiles to detect TiO_2 films on the plates. When applying heat treatment at 773 K in air to the Ti plate, the EDS result shows the remarkable increase in the oxygen content at the plate surface. The TiO_2 formation at the surface is clearly detected, and the

thickness is quite large compared to the as-received one. This annealed Ti plate was applied to the wettability evaluation as the substrate. Fig. 10 shows the variation of the diameter, height and contact angle as a function of time in the wetting test at 1073 K using the annealed pure Ti substrate shown in Fig. 8b. The photos of the changes in the droplet outline are also shown in Fig. 10. They are completely modified by the above equations to consider the Mg evaporation phenomenon in the droplet outline during the test. Comparing this with the above result shown in Fig. 7b, there are two remarkable differences in the wetting phenomena between them: (i) the dependence of the contact angle on the time (wetting behavior); and (ii) the contact angle value in the stable state (wettability). Concerning (i), the profile of the contact angle consists of three characteristic regions. The first indicates that the contact angle is nearly constant at 110° for a short period of about 180 s (A). The second indicates a sudden decrease in the contact angle with a sharp slope (B). The third is typified by a gradual decrease, with a contact angle close to 68° (C). The diameter and height of the molten droplet also indicate the similar behavior to the contact angle change as mentioned above. In particular, they are almost constant for 180 s after starting the test. This means no progress of the wetting phenomenon of pure Mg molten droplets on annealed Ti substrate at 1073 K. After that, a drastically spreading diameter with time is observed, and the diameter gradually increases due to the wetting phenomenon. Concerning the difference in the contact angle profile using as-received pure Ti substrate and annealed substrate, the above result suggests the possible effect of TiO_2 surface films on the wettability of pure Mg. An additional experimental approach was carried out using TiO_2 ceramic substrate (98.2% purity) instead of pure Ti to evaluate the

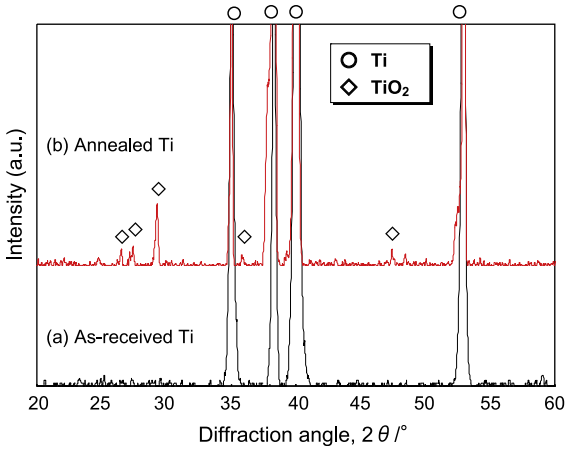

Fig. 9. XRD profiles of as-received pure Ti substrate (a) and annealed at 773 K for 3.6 ks in air (b).

contact angle behavior during the initial period. Fig. 11 shows the changes in the diameter, height and contact angle of a molten pure Mg droplet on TiO_2 substrate at 1073 K as a function of time; the Mg evaporation phenomenon is considered for changes in each parameter. The height and diameter show a very slight decrease, and the contact angle is almost constant at about 82°. This means the wettability of TiO_2 by pure Mg is inferior to that of pure Ti by pure Mg at the same temperature shown in Fig. 7b. In addition, the constant contact angle indicates that the interfacial phenomenon during wetting is stable and occurs uniformly at the contact area between the Mg droplet and the TiO_2 substrate. Fig. 12 shows the EMPA result at the interface between a solidified pure Mg droplet and the TiO_2 substrate. SEM–EDS observation was also carried out on areas (A) and (B) of the TiO_2 plate. The

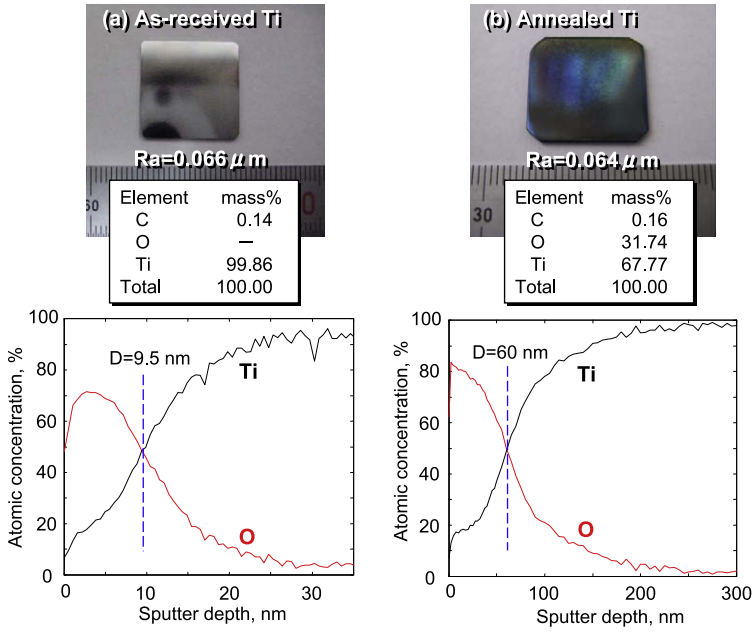

Fig. 8. Appearance of as-received pure Ti substrate (a) and annealed at 773 K for 3.6 ks in air (b), and EDS and AES results on each substrate.

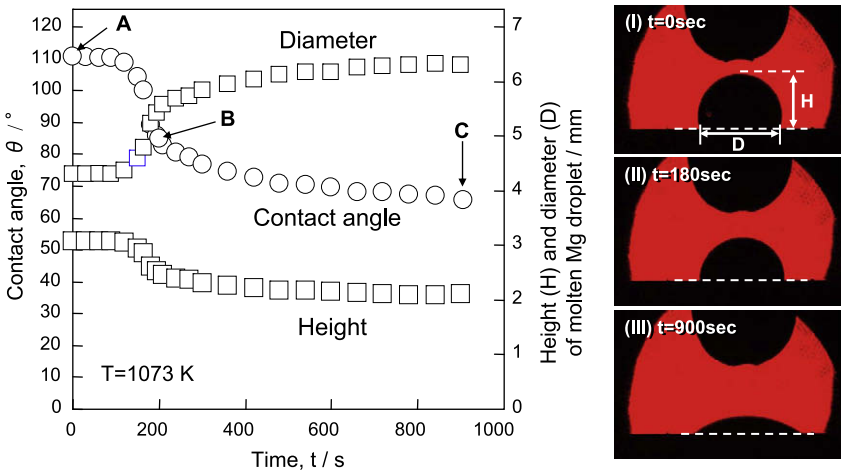

Fig. 10. Changes in modified morphological parameters by considering Mg evaporation effect in measuring wettability of annealed pure Ti plate by molten pure Mg at 1073 K.

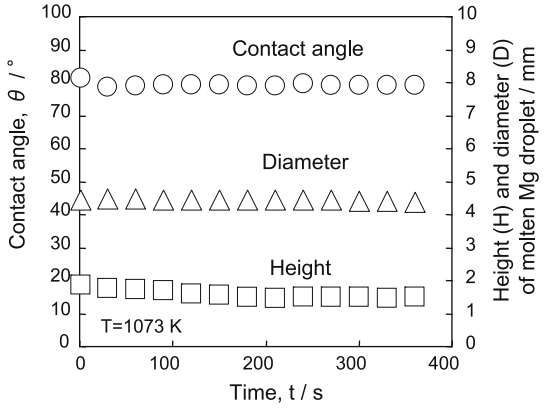

Fig. 11. Changes in contact angle, modified diameter and height of pure Mg droplet on TiO_2 ceramic substrate at 1073 K as a function in time.

reacted layer, about 100 μm thick, is observed at the surface of the TiO_2 plate, and Mg diffusion into the TiO_2 occurs. However, no Ti element is detected in the solidified Mg droplet because there is no solution of Ti into Mg as shown in the Mg–Ti binary phase diagram [23]. SEM–EDS analysis indicated that the TiO_2 grain boundaries are very sharp and obviously observed at area (A), where no Mg is detected. Several small original pores less than about 1 μm are also observed. This means that TiO_2 at area (A) is an as-received original material, and does not react with the pure Mg during the wetting test. On the other hand, area (B) reveals quite different microstructures from that in the area (A). For example, the small original pores shown in area (A) are not observed, and Mg elements are infiltrated into the pores at the boundaries. The TiO_2 grain boundaries are not smooth, but uneven. Some fine particles with a diameter of 500 nm or less are observed around the TiO_2 primary grains. When considering the very high reactivity of Mg with TiO_2 as shown in the Eq. (7), the reduction of TiO_2 occurs in area (B) during the wetting test. In considering the profiles of the contact angle of the pure Mg droplets on the as-received Ti (Fig. 7b) and TiO_2 ceramic substrate (Fig. 11), the constant contact angle at the initial period for 180 s shown in Fig. 10 depends on the reduction of the thicker TiO_2 surface films by molten pure Mg droplets.

On the other hand, concerning the difference in the contact angle using the as-received Ti and annealed one coated with thicker TiO_2 films, the contact angle of the latter at the stable state is about 68°. It is much larger than that using as-received Ti plate ($\theta = 31°$) shown in Fig. 7b. Fig. 13 shows the SEM–EDS analysis results on the cross-section at the interface between solidified pure Mg droplet and Ti substrate. It is obvious that the surface roughness of the as-received Ti plate is smooth (a), and the annealed one reveals uneven surfaces (b), although both plates before the wetting test have a very smooth surface with a roughness of 61–67 nm. In addition, Mg and O elements are concentrated at the interface of the nearest surface area (about 1–3 μm depth) of the Ti plate as shown in Fig. 13b. The increment in the surface roughness is due to the reduction of TiO_2 films, and this morphological change is similar in the case of the TiO_2 ceramic plate as shown in Fig. 12. It has been reported that the surface roughness of the substrate affects the wetting phenomenon [24–26]. Its effect is considered in the Young's equation by using the roughness factor, r (r = the ratio of the actual area of a rough surface to the geometric projected area). The modified Young's equation gives a new contact angle by considering the surface roughness effect, θ_w ($\cos\theta_W = r\cos\theta$; r = roughness factor). This is based on the assumption that the liquid completely penetrates into the roughness grooves. In this study, the SEM–EDS analysis results shown in Figs. 12 and 13 indicate that the molten Mg droplet also completely penetrates into the Ti and TiO_2 plate surface. Therefore, the above modified Young's equation can be applied in discussion of the effect of surface roughness on the wettability. In general, a rough surface means $r > 1$, and $r = 1$ indicates a smooth surface. In the case of $r > 1$, the interfacial energy γ_{SL}, meaning that for solid–liquid (substrate–molten drop-

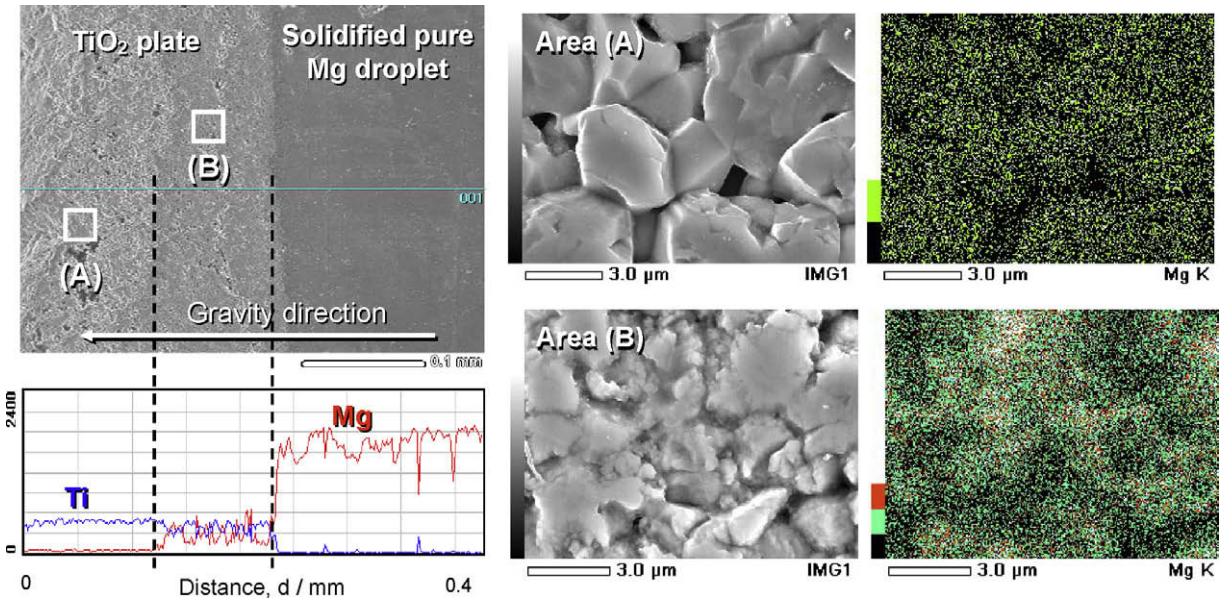

Fig. 12. EPMA analysis on interface between solidified pure Mg droplet and TiO_2 plate after wetting test at 1073 K, and SEM–EDS observation at area (A) and (B) in TiO_2 ceramic substrate.

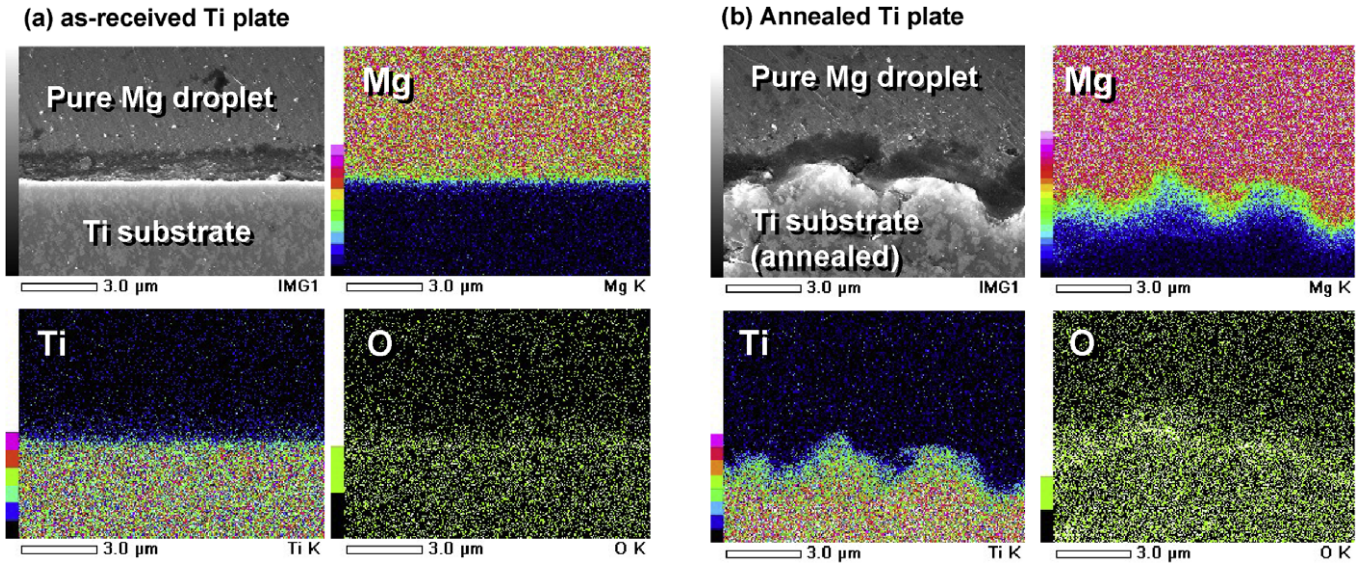

Fig. 13. SEM–EDS observation on interface of solidified pure Mg droplet on as-received (a) and annealed pure Ti plate (b) after wetting test at 1073 K.

let), increases. This results in the decrease of $\cos\theta$ in Young's equation. That is, the contact angle θ increases, indicating a poor wettability by the rough surface of the substrate. Accordingly, the wetting phenomenon of pure Ti by molten pure Mg at high temperature is schematically illustrated in Fig. 14. The profile of the contact angle as a function of time consists of three typical regions: constant value at the initial period (region I); sudden decrease in contact angle (region II); and gradual decrease with a gentle slope and stable value (region III). Region (I) is mainly due to the wetting behavior of pure Mg by the original TiO_2 surface films of coating on the Ti substrate. Therefore, the stable period depends on the thickness of such oxide layers. In region (II), wetting of pure Mg by TiO_2 films occurs as well newly created pure Ti via reduction. The contact angle strongly depends on the area ratio of TiO_2 films to pure Ti, and decreases with increase in the contact area with pure Ti. The contact angle in region (III) is mainly governed by the wettability of pure Ti by pure Mg molten droplet. At the edge of the Mg droplet, the wetting phenomenon of Mg by TiO_2 surface layers is also effective. However, its influence on the contact angle is very limited. Concerning the significantly large difference of the contact angle of about 37° between as-received Ti and annealed Ti, the uneven surface roughness due to the reduction of TiO_2 films by molten Mg shown in Fig. 13b prevents the surface tension (γ_{SL}), and the contact angle increasing markedly.

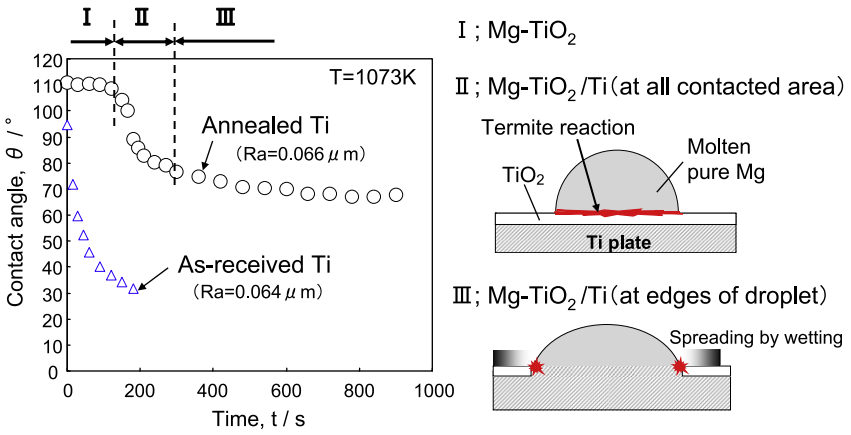

Fig. 14. Effect of TiO_2 thin film of pure Ti plate on changes in contact angle between molten Mg droplet and Ti plate at 1073 K.

The results in the present study have clarified that Ti has a good wettability by molten Mg droplets. This strongly supports that ultrasonic treatment for grain refinement of molten Mg alloys, described in a previous study [27], is more efficient using a Ti sonotrode, which effectively transmits the ultrasonic energy into the molten Mg, compared to the chemical approaches using the addition of carbon or aluminum carbides. Therefore, the wettability analysis between Ti plate and molten Mg droplets is very important for material design to develop advanced composites with refined microstructures.

4. Conclusions

The wettability of pure Ti by molten pure Mg was evaluated by the sessile drop method to fabricate Mg matrix composites reinforced with Ti particulates. The contact angle was measured in high-purity argon (99.999%) at 1073 K. To eliminate the Mg evaporation phenomenon in estimating the true contact angle, the calculation method adopted modified morphological parameters such as height and diameter of the molten pure Mg droplet on the Ti substrate. By considering its evaporation effect, the equilibrium contact angle was 31°, and an increment of 11° was obtained, compared to the original contact angle without consideration of Mg evaporation. This was much smaller than that using TiC and SiC as the substrate. Hence the wettability between Mg and Ti was very good compared to conventional ceramics used as reinforcements of Mg composites. The effect of the surface oxide films of the Ti plate was discussed by employing as-received Ti plate, air-annealed Ti plate and TiO_2 ceramic plate as the substrate. The reduction of the TiO_2 layer contacting the molten Mg determined the initial contact angle of 95–110°, which was much higher than the equilibrium value. When Mg contacted pure Ti area after reduction, the contact angle suddenly decreased.

References

[1] Ferkel H, Mordike BL. Mater Sci Eng A 2001;298:193.
[2] Gupta M, Lai MO, Saravanaranganathan D. J Mater Sci 2000;35:2155.
[3] Wang HY, Jiang QC, Li XL, Wang JG. Scripta Mater 2003;48:1349.
[4] Hassan SF, Tan JJ, Gupta M. Mater Sci Eng A 2008;486:56.
[5] Hassan SF, Gupta M. Mater Sci Eng A 2005;392:163.
[6] Smithells CJ. Metals Reference Book. 7th ed. London: Butterworth; 1992. p. 173.
[7] Properties and Selection. Non-Ferrous Alloys and Special-Purpose Materials. In: ASM Handbook, vol. 2. Materials Park, OH: ASM International 1990.
[8] Hassan SF, Gupta M. J Alloy Compd 2002;345:246.
[9] Xi YL, Chai DL, Zhang WX, Zhou JE. Mater Lett 2005;59:1831.
[10] Xi YL, Chai DL, Zhang WX, Zhou JE. Scripta Mater 2006;54:19.
[11] Froumin N, Frage N. Acta Mater 2000;48:1435.
[12] Contreras A, Bedolla E, Perez R. Acta Mater 2004;52:985.
[13] Young T. Philos Trans R Soc London 1805;95:65.
[14] Leon CA, Lopez VH, Bedolla E, Drew RAL. J Mater Sci 2002;37:3509.
[15] Muscat D, Drew RAL. Metall Mater Trans 1994;25A:2357.
[16] Contreras A, Leon CA, Drew RAL, Bedolla E. Scripta Mater 2003;48:1625.
[17] Fujii H, Izutani S, Matsumoto T, Kiguchi S, Nogi K. Mater Sci Eng A 2006;417:99.
[18] Dushman S, Lafferty JM. Scientific Foundations of Vacuum Science. 2nd ed. New York: John Wiley; 1962. p. 173.
[19] Zhao H, Debroy T. Metall Mater Trans B 2001;32:163.
[20] Hatch JE. Aluminum, properties and physical metallurgy. Metals Park, OH: American Society for Metals 1984.
[21] Gaskell DR. Introduction to metallurgical thermodynamics. New York: Hemisphere; 1981. p. 287.
[22] Ellingham HJT. J Soc Chem Ind 1944;63:125.
[23] Murray JL. Phase Diagrams of Binary Titanium Alloys. Materials Park, OH: ASM International 1998.
[24] Wenzel RN. Ind Eng Chem 1936;28:988.
[25] Wenzel RN. J Phys Chem 1949;53:1466.
[26] Marmur A. R Soc Chem Soft Matter 2006;2:12.
[27] Ramirez A, Qian Ma, Davis B, Wilks T, StJohn DH. Scripta Mater 2009;59:19.